Nature of Monster Sawteeth and Their Relationship to Alfvén Instabilities in Tokamaks

S. Bernabei,[1] M. G. Bell,[1] R. V. Budny,[1] E. D. Fredrickson,[1] N. N. Gorelenkov,[1,2] J. C. Hosea,[1] R. Majeski,[1] E. Mazzucato,[1] C. K. Phillips,[1] G. Schilling,[1] and J. R. Wilson[1]

[1]*Princeton Plasma Physics Laboratory, Princeton, New Jersey 08543*

[2]*TRINITI, Troitsk, Moscow, Russia 142092*

(Received 19 May 1999; revised manuscript received 10 August 1999)

A correlation is explored between the presence of energetic particle modes (EPM) and long-period sawtooth oscillations in tokamak plasmas heated by rf waves. The eventual crash of these sawteeth is explained in terms of the loss of the stabilizing fast particles due to the EPM. The absence of long-period sawteeth in high q_a discharges is explained in terms of ion loss due to toroidal Alfvén eigenmodes.

PACS numbers: 52.50.Gj, 52.55.Fa

The confinement in tokamak plasmas of energetic particles, either formed by auxiliary heating systems or by nuclear reactions, is of central importance to magnetic fusion experiments. Alfvén instabilities may be excited by energetic particles and can also cause the loss of these particles. Energetic ions can also produce stabilization of the ubiquitous sawtooth instability.

High-power plasma heating by waves in the ion cyclotron range of frequency (ICRF) which couple to a minority ion species creates a fast ion distribution in the plasma [1]. It has been observed that when this hot-ion component is created inside of the radius where $q = 1$, $r_{q=1}$, it lengthens the sawtooth period, as predicted theoretically [2,3]. In TFTR [4] and other tokamaks it has been observed that the length of the sawtooth period varies with plasma conditions. Very interestingly, both long and ultralong (monster) sawteeth can be observed in the same discharge (Fig. 1). The occurrence of monster sawteeth depends on the minority-ion concentration, the ICRF resonance location, and, most interestingly, the value of q at the edge, q_a. Specifically, in TFTR, monster sawteeth are observed at $q_a \leq 3.6$, with a ICRF power $\geq$2.8 MW. Monster sawteeth in TFTR are always accompanied by the destabilization of Alfvén instabilities [5,6] (Fig. 2). In this Letter we discuss the correlation between these two phenomena and postulate that the termination of the long sawtooth-free period is due to depletion of stabilizing ions from the core of the plasma by the Alfvén instabilities.

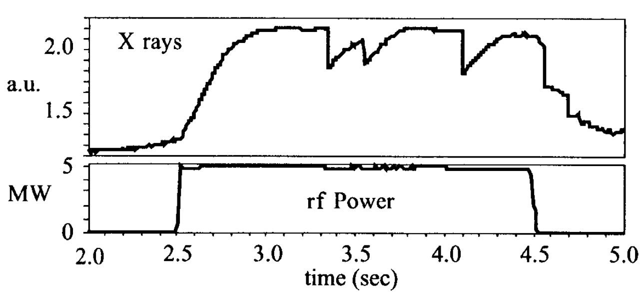

FIG. 1. X-ray signal showing two monster sawteeth and a shorter one; the last sawtooth is due to the rf power termination. $I_p = 1.68$ MA, $B_T = 3$ T, and $q_a = 3.2$.

These experiments were conducted in TFTR in deuterium plasmas with few percent hydrogen minority. The parameter ranges were density $(2-4.6) \times 10^{19}$ m^{-3}, plasma current 1.2–1.8 MA, toroidal field 3.0–4.5 T, and ICRF frequencies 43, 47, and 63.6 MHz with power up to 11 MW. The q_a ranged from 2.8 to 6.8.

It has been demonstrated that Alfvén instabilities are responsible for degradation of the ICRF heating efficiency in these TFTR discharges [5]. There are two kinds of instabilities observed in the Alfvén frequency range [7]. One is readily identified as the toroidal Alfvén eigenmode (TAE), by the dependence of its frequency on density. The other has a rapidly changing (chirping) frequency. Figure 3 shows the Alfvén spectrum of fluctuations detected by a reflectometer (a) and by a Mirnov loop (b) [7]. The reflectometer, which is aimed at the core of the plasma, detects the chirping modes before the Mirnov loop, which is mounted outside the plasma. For a brief period the mode measurements overlap, indicating that the two instruments are detecting the same mode. This sequence suggests that the chirping modes are initially core localized, but as plasma conditions evolve, they move outside the region covered by the reflectometer and start being

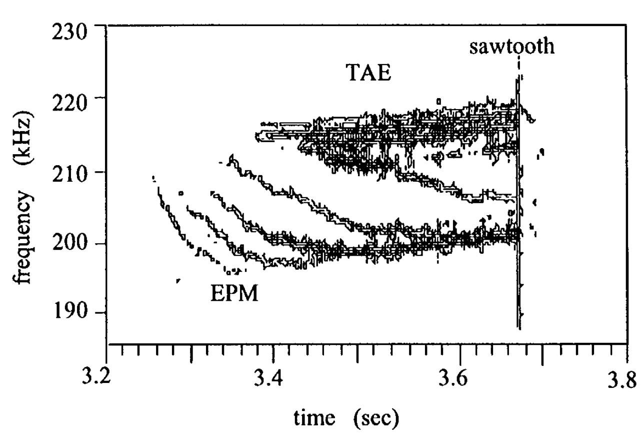

FIG. 2. TAE and EPM from a magnetic probe, preceding a monster sawtooth at $t = 3.67$ sec, $q_a = 3.2$, and $P_{\rm rf} = 5.2$ MW.

 0031-9007/00/84(6)/1212(4)$15.00

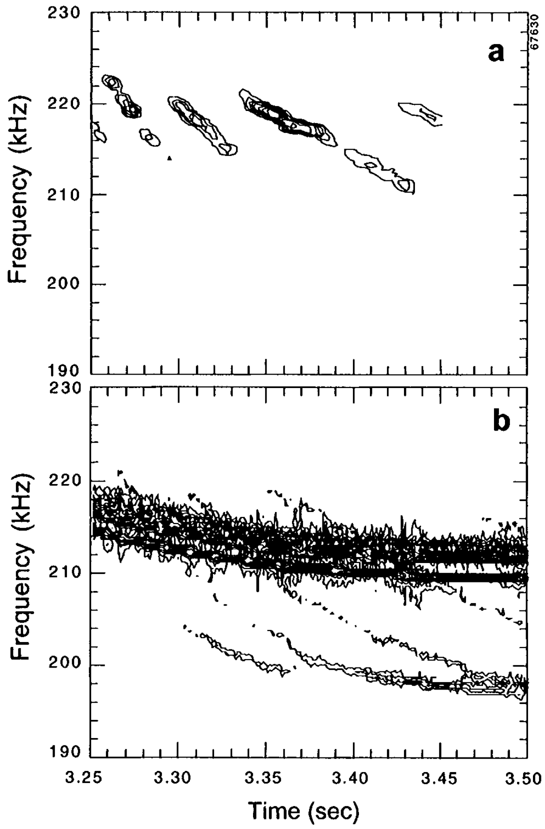

FIG. 3. Alfvén spectra, detected by reflectometry in the core (a) and by Mirnov loops at the edge (b). The Mirnov signal includes TAE ($210 \leq f \leq 220$ kHz) which are absent from the reflectometer signal.

detected by the Mirnov coil. These chirping modes are observed to trigger fast ion losses [5].

Analysis with the NOVA-K code [8] fails to predict these chirping modes, but the nonperturbative code HINST [9] finds a branch of shear Alfvén waves corresponding to the energetic particle modes (EPM) predicted by theory [10], also called resonance TAE (RTAE) [11]. The analysis with HINST indicates that these modes should be localized to the core, where they are driven by the strong energetic minority-ion pressure gradient and reside in the Alfvén continuum. The position of the mode near the core is determined by the minor radius where the safety factor is $q = q_{\mathrm{TAE}} \approx 1 - \frac{1}{2n}$, where n is the toroidal mode number, since these modes are close to TAE, although modified by the strong drive. Thus as the central q, q_0, decreases due to the resistive current diffusion, the EPM location should move radially outward, in agreement with the experiment [5]. As the q_0 decreases, high n-number modes will appear first, since for these q_{TAE} is closer to 1. The radial dependence of the EPM frequency is shown in Fig. 4(a). In Fig. 4(b) we show the frequency calculated by HINST for several EPMs as a function of q_0. The abscissa has been reversed to show the similarity of the frequency behavior with that of Fig. 3, since q_0 decreases approximately linearly in time between the sawtooth

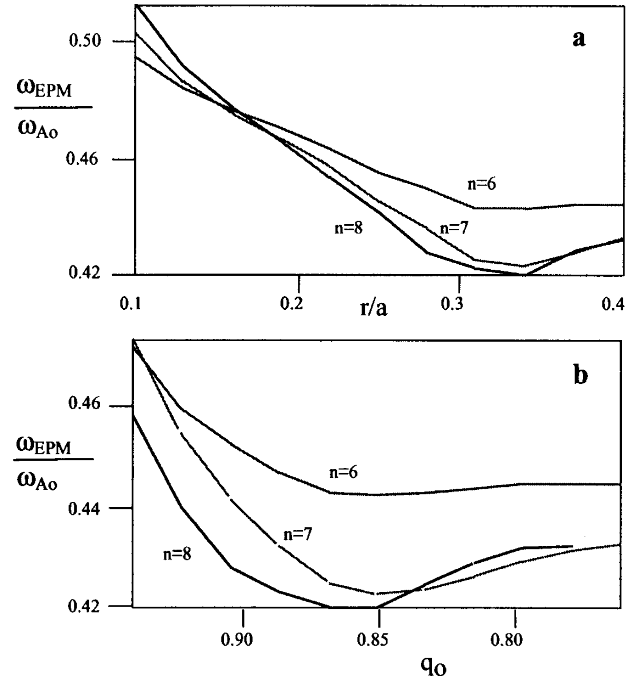

FIG. 4. Variation of the EPM frequency calculated by HINST, normalized to the value of the central Alfvén frequency at $q_0 = 0.9$ as a function of radius (a) and vs decreasing q_0 (b).

crashes. At high n numbers q_{TAE} for different modes are close to each other so that we can expect the excitation of several modes at the same time if they are located near the strong fast particle pressure gradient domain.

We carried out simulations with the ORBIT code [12] of the interaction of a representative population of energetic particles with the perturbed field of the modes deduced from the Mirnov loops and reflectometer signals. Two conditions were identified which lead to fast particle losses: either the mode is global (in the sense that it extends throughout the plasma cross section) or it changes radial location, inducing a transport of fast particles with it.

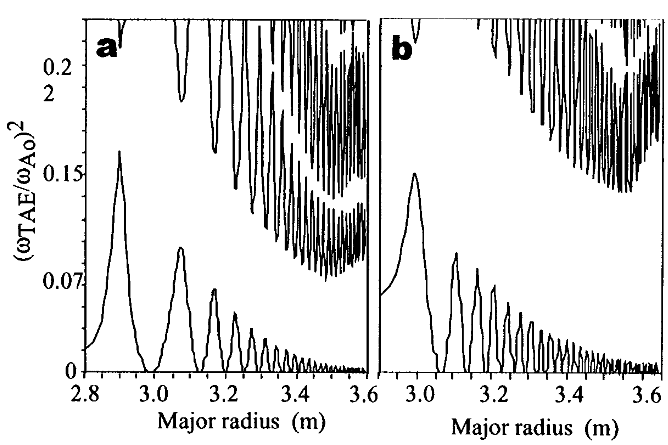

FIG. 5. Alfvén frequency gap calculated by NOVA-K for a discharge with $q_a = 3.2$ (a) and $q_a = 4.5$ (b).

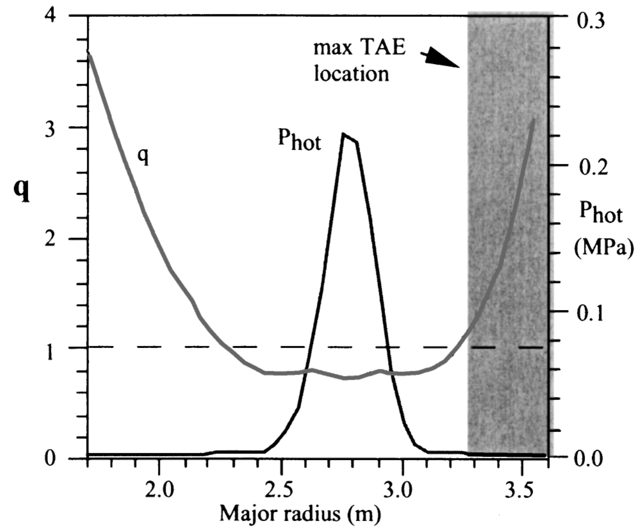

FIG. 6. TRANSP calculation of the q profile and of the hot-ion pressure generated by ICRF heating, $q_a = 3.2$ and $P_{\mathrm{rf}} = 6.2$ MW.

In previous experiments, loss of sawtooth stabilization was explained by widening of the $r_{q=1}$ radius until the average hot-ion pressure within it was no longer sufficient for stabilization of the $m = 1$ mode. A deficiency of this explanation is that the stabilization occurs at low q_a where the $r_{q=1}$ is fairly large and not at high q_a where it is much smaller. At the same time it is also puzzling that the EPMs appear earlier in time than the TAE, considering that the hot-ion pressure gradient required to destabilize the EPMs is higher due to strong continuum damping.

The solution of these puzzles rests in the relative spatial location of the EPM and TAE. At low q_a, the structure of the Alfvén spectrum produces an Alfvén frequency gap narrow enough to restrict the TAE to the outer half of the plasma, or more importantly away from the core where the fast ion distribution is formed. Figure 5 shows the comparison between the gap calculated at $q_a = 3.2$ (same conditions as Fig. 1) and at $q_a = 4.5$.

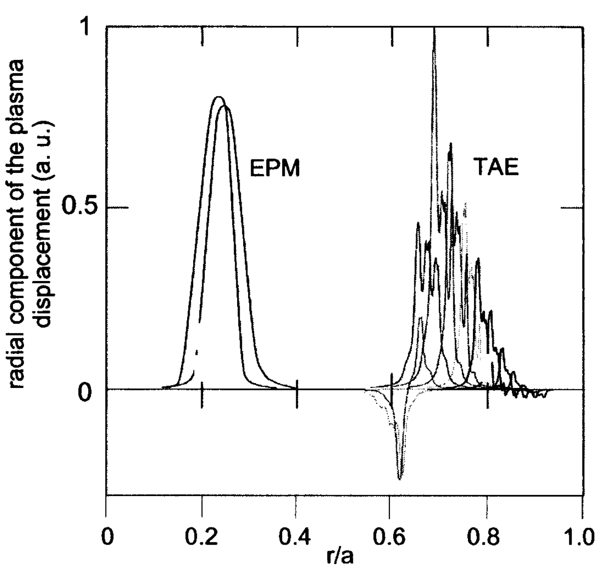

FIG. 7. Reconstruction of the eigenfunctions for the modes with $n = 8$ EPM and TAE from HINST and NOVA-K for $q_a = 3.2$, for the same experimental conditions of Figs. 4, 5(a), and 6.

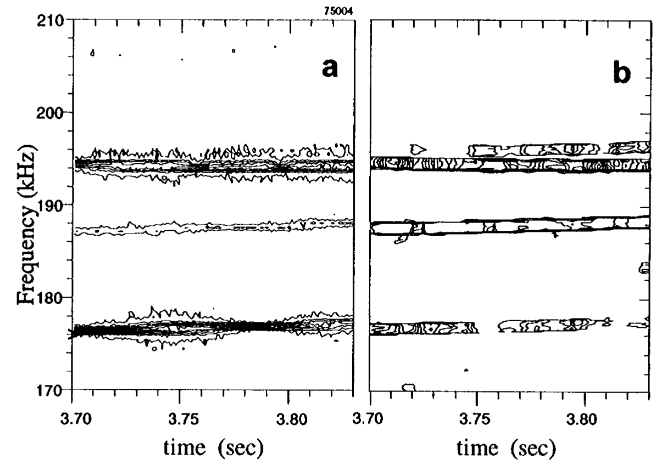

FIG. 8. Alfvén spectra from Mirnov loop (a) and from reflectometry (b) in a discharge with $q_a = 4.5$. TAE are detected both in the core and at the edge.

The fast ion distributions in both cases are calculated with the ICRF package of TRANSP [13]. For $q_a = 3.2$ the entire fast ion distribution is formed well inside the $r_{q=1}$ and does not overlap with the region where TAEs can exist (Fig. 6). This is also evident from Fig. 3 which shows that the reflectometer does not detect the TAE in the core. This is confirmed by HINST analysis, which agrees with the NOVA gap structure that the TAE eigenfunctions are contained within the gap with very little penetration into the continuum. The relative radial location and structure of the modes is shown in Fig. 7. In this situation, aside from fishbonelike $n = 1$ burst modes which are responsible for minor radial transport [5], no other loss mechanism is present to deplete the fast ion distribution. This

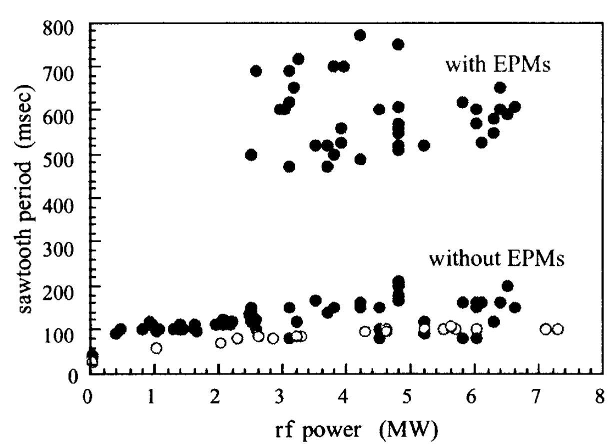

FIG. 9. Sawtooth period versus rf power. Full circles are at $q_a = 3.2$, open circles at $q_a = 4.5$.

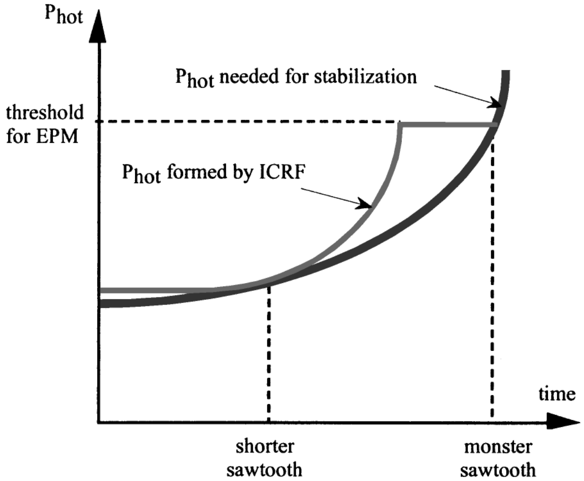

FIG. 10. Scenario showing that P_{hot} generated by ICRF heating initially approaches the value required for stabilization of the sawtooth, then grows faster providing a good margin for stability until its growth is clamped by the onset of EPM. Shorter sawtooth refers to the lower points in Fig. 9.

allows the formation of a population of fast particles strong enough to stabilize the sawtooth for a long time. However, the very same population can form a radial pressure gradient large enough to destabilize the EPM. If conditions evolve in such a manner that the location of the EPM is shifted outward (as in the case of decreasing q_0), fast particles are transported radially. When the depletion of fast ions inside $r_{q=1}$ becomes too severe, not enough fast ions are left to stabilize the sawtooth and a giant crash occurs.

Conversely, at high q_a, because of the steep gradient of the q profile, the Alfvén gap widens enough to bring the TAE in contact with the fast ion population being created in the core. Figure 8 shows again the comparison between the Mirnov loop and the reflectometer signals. It is seen that the same TAEs are detected at the edge and in the core. In this situation, as the fast ion population is formed by ICRF, it is depleted by the TAE. Therefore, a population of fast ions cannot be built up to the level required for sawtooth stabilization or for eventual EPM destabilization.

Figure 9 shows the sawtooth period vs rf power. At low q_a there are two groups of sawteeth, some which are lengthened by a factor of $\sim$4 and others by a factor of $\sim$20. There are no points in between, indicating a bifurcation. The scenario shown schematically in Fig. 10 could explain this. As time progresses two events happen in parallel: the hot ion pressure (P_{hot}) in the core starts increasing while q_0 decreases, widening $r_{q=1}$. It appears that at the beginning there is a period of marginal stability during which the few losses due to the fishbonelike burst modes could cause a sawtooth crash. The heavy line represents the required P_{hot} for stabilization and the almost parallel line the increase of P_{hot} with ICRF heating. If the critical initial phase is passed, there is ample fast ion population for sawtooth stabilization, as shown by the fact that there is a period of $\sim$200 msec during which heavy ion losses are observed before the crash. Previously it has been assumed that at this point the sawteeth are stable until $r_{q=1}$ widens sufficiently so that the fast ion population is no longer sufficient for stabilization. If this was the case the long period shown in Fig. 9 should increase with power instead of being nearly independent of power.

This work was supported by U.S. Department of Energy Contract No. DE-AC02-76CH03073.

[1] J.R. Wilson *et al.*, in *Plasma Physics and Controlled Nuclear Fusion Research 1992, Proceedings of the 14th International Conference, Würzburg, 1992* (International Atomic Energy Agency, Vienna, 1993), Vol. 1, p. 661.
[2] D.J. Campbell *et al.*, Phys. Rev. Lett. **60**, 2148 (1988).
[3] R.B. White *et al.*, Phys. Plasmas **2**, 2871 (1995).
[4] R. Hawryluk *et al.*, Plasmas Phys. Controlled Fusion **33**, 1509 (1991).
[5] S. Bernabei *et al.*, Phys. Plasmas **6**, 1880 (1999).
[6] L.-G. Ericksson *et al.*, Phys. Rev. Lett. **81**, 1231 (1998).
[7] E.D. Fredrickson *et al.*, Nucl. Fusion **35**, 1457 (1995).
[8] C.Z. Cheng, Phys. Rep. **211**, 1 (1992).
[9] N.N. Gorelenkov, C.Z. Chang, and W.M. Tang, Phys. Plasmas **5**, 3389 (1998).
[10] F. Zonca and L. Chen, Phys. Plasmas **3**, 323 (1996).
[11] C.Z. Cheng, N.N. Gorelenkov, and C.T. Hsu, Nucl. Fusion **35**, 1639 (1995).
[12] R.B. White and M.S. Chance, Phys. Fluids **27**, 2455 (1984).
[13] R.V. Budny *et al.*, Nucl. Fusion **35**, 1497 (1995).